JCAMECH

Vol. 50, No. 1, June 2019, pp 69-75
DOI: 10.22059/jcamech.2019.279153.384

Vibration suppression analysis for laminated composite beams contain actuating magnetostrictive layers

Ashraf M. Zenkour[a,b,] and Hela D. El-Shahrany[b,c]*

[a] *Department of Mathematics, Faculty of Science, King Abdulaziz University, P.O. Box 80203, Jeddah 21589, SAUDI ARABIA*
[b] *Department of Mathematics, Faculty of Science, Kafrelsheikh University, Kafrelsheikh 33516, EGYPT*
[c] *Department of Mathematics, Faculty of Science, Bisha University, Bisha, SAUDI ARABIA*

ARTICLE INFO

Article history:
Received: 13 April 2019
Accepted: 28 April 2019

Keywords:
Laminated Composite Beam
Vibration Control
Velocity Feedback Control
Magnetostrictive Material
Shear Deformation Theory

ABSTRACT

This paper presents the analysis of vibration control of a laminated composite beam that including magnetostrictive layers. The formulation of problem is presented based on the shear deformation beam theory. For vibration suppression, the velocity feedback control with constant gain distributed is considered. Navier's method is applied to analyze the solution of vibration suppression of laminated beam with the simply-supported boundary conditions. The influence of lamination schemes, modes, number of smart layers at the structure, the control gain of the magnetic field intensity and smart layer position on suppress of the vibration are discussed. In addition, the controlled motion of some special laminated composite beam is tested.

1. Introduction

The magnetostrictive materials are one of common smart materials that used as actuators and sensors, where it has the properties of being change its distances in response to the magnetic field. Examples of magnetostrictive materials are cobalt, iron, nickel, ferrite, and Terfenol-D. A magnetostrictive material able to product strains up to $2500\,\mu m$ and high energy density $2.5 \times 10^4\ J/m^3$ in reaction to stresses of the applied magnetic field [1]. Therefore, the magnetostrictive materials are used to control of systems vibration. In this part, some articles are introduced to know about this topic's background.

The design and theoretical researches about active control of laminated composite beams/plates including actuators of smart magnetostrictive materials have been investigated [2-17]. Pratt and Flatau [18] designed and analyzed a self-sensing magnetostrictive actuator according to the linear model of Terfenol-D magnetostrictive transduction. Anjanappa and Bi [19, 20] discussed the feasibility of smart structural applications that contain magnetostrictive mini actuators. Under effect of a magnetic field and an external follower force, Arani et al. [21] studied the magnetostrictive smart plate (MsP) vibration. Thick laminated composites with integrated sensors and actuators are studied based on the third-order plate theory of Reddy [22]. In addition, Koconis et al. [23] used actuators to control the composite plates and shells shape. Shankar [24] has studied the hygrothermal effect of delaminated composite plates embedded active fiber composite (AFC) sensor and actuators. Arani et al. [25] discussed the free vibration of rectangular magnetostrictive plate supported by elastic foundation with applying a feedback control system according to trigonometric shear deformation theory of high order. Li et al. [26] investigated random vibration suppression for laminated composite plates with piezoelectric fiber reinforced composite layer on the top. Li and Narita [28] used the Piezoelectric-fiber-reinforced composites (PFRCs) patches as actuator and discussed the effect of the PFRCs patches on vibration suppression of laminated composites plate subjected to arbitrary boundary conditions. Song et al. [29] used smart actuators and sensors to control the E-glass/epoxy laminated composite beam. Kim et al. [30] analyzed the dynamic response of surface bonded macro fiber composite actuators for an end-capped cylindrical shell.

In the present study, control of the laminated composite beam response that contain magnetostrictive material layers, which used as sensors or actuators, is studied using a shear deformation beam theory without require shear correction factor [27]. For actively control the dynamic reaction of the system, a simple velocity feedback control through a close-loop control is utilized. The governing equations of motion are derived through the principle of Hamilton and Navier's method is applied to obtain the solution. Some effects are investigated such as lamination scheme, modes, number of smart layers at the structure, location of the smart material layer and control gain coefficient on system vibration suppression. Farajpour [38] analyzed the nonlinear free vibration for magneto-electro-elastic nanoplates and studied various non-classical plate theories.

2. Formulation of the Problem

Suppose that a sandwich-laminated beam with top and bottom smart magnetostrictive layers and the remaining $(k-2)$ layers

* Corresponding Author: zenkour@gmail.com

also embedded the mth and $(k-m+1)$th magnetostrictive material with Terfenol-D particles where $m \neq 1$, k as shown in Figure 1. The remaining $k-4$ layers can be made using carbon fiber reinforced polymeric (CFRP) material. The problem of vibration suppression in these beams based on the shear deformation beam theory contains only two unknown functions where does not require shear correction factor.

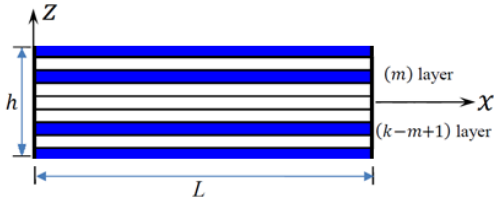

Figure 1. Schematic diagram of the beam

The displacement field can be assumed as [27]

$$\begin{aligned} u(x,y,z,t) &= -z\frac{\partial w_0}{\partial x} + h_1(z)\varphi(x,t), \\ v(x,y,z,t) &= 0, \\ w(x,y,z,t) &= w_0(x,t), \\ h_1(z) &= h\sinh\left(\frac{z}{h}\right) - \frac{4z^3}{3h^2}\cosh\left(\frac{1}{2}\right). \end{aligned} \tag{1}$$

The simple sinusoidal beam theory [27, 31-37] is obtained when $h_1(z) = (h/\pi)\sin(\pi z/h)$ and the same results almost are given. In Eq. (1), $w_0(x,t)$ indicates the transverse deflection while the function $\varphi(x,t)$ represents the rotation about y-axis. Both w_0 and φ are unknown functions to be determined.

The strain-displacement components are displayed as

$$\varepsilon_{xx} = z\varepsilon_{xx}^{(1)} + h_1(z)\varepsilon_{xx}^{h}, \quad \gamma_{xz} = h_2(z)\gamma_{xz}^{h}, \tag{2}$$

where

$$\begin{aligned} &\varepsilon_{xx}^{(1)} = -\frac{\partial^2 w_0}{\partial x^2}, \quad \varepsilon_{xx}^{h} = \frac{\partial \varphi}{\partial x}, \\ &\gamma_{xz}^{h} = \varphi, \quad h_2(z) = h_1'(z). \end{aligned} \tag{3}$$

The stress-strain relations for a linear fiber-reinforced kth layer are represented as

$$\sigma_{xx}^{(k)} = \bar{Q}_{11}^{(k)}\varepsilon_{xx}, \quad \sigma_{xz}^{(k)} = \bar{Q}_{55}^{(k)}\gamma_{xz}. \tag{4}$$

The stress-strain relations for a magnetostrictive layer is represented as

$$\sigma_{xx}^{(m)} = \frac{1}{S_{11}^{(m)}}\left(\varepsilon_{xx} - d_{31}^{(m)}H\right) \equiv \bar{Q}_{11}^{(m)}\varepsilon_{xx} - \bar{e}_{31}^{(m)}H, \tag{5}$$

where H is the magnetic field intensity, $d_{31}^{(m)}$ is the magneto-mechanical coupling coefficient, $E_{11}^{(m)}$ is the magnetostrictive layer modulus ($\bar{e}_{31}^{(m)} = \bar{Q}_{11}^{(m)}d_{31}^{(m)}$) and $S_{11}^{(m)}$ denotes the mth magnetostrictive layer compliance

$$S_{11}^{(m)} = \frac{1}{E_{11}^{(m)}} = \frac{1}{Q_{11}^{(m)}}, \tag{6}$$

In addition, the coefficients $\bar{Q}_{ij}^{(k)}$ are given in Appendix A.

3. Velocity Feedback Control and Governing Equations

Suppose a simple velocity proportional closed-loop feedback control. The relationship between the magnetic field intensity H and coil current I can be obtained as [2]

$$\begin{aligned} H(x,t) &= k_c I(x,t), \\ I(x,t) &= c(t)\frac{\partial w_0}{\partial t}, \end{aligned} \tag{7}$$

where k_c is the coil constant and $c(t)$ is the control gain. The relationship between the coil constant k_c, the coil width b_c, the coil radius r_c, and the turns number in the coil n_c is expressed as

$$k_c = \frac{n_c}{\sqrt{b_c^2 + 4r_c^2}}. \tag{8}$$

Equations of motion can be obtained due to Hamilton principle. That is

$$\begin{aligned} 0 = &\int_0^T\int_0^L\int_A\left[\sigma_{xx}\left(z\delta\varepsilon_{xx}^{(1)} + h_1(z)\delta\varepsilon_{xx}^{h}\right) + \right. \\ &\left.\sigma_{xz}h_2(z)\delta\gamma_{xz}^{h}\right]\mathrm{d}A\mathrm{d}x\mathrm{d}t - \int_0^T\int_0^L\int_A\rho\left[\left(-z\frac{\partial \dot{w}_0}{\partial x} + \right.\right. \\ &\left.\left.h_1(z)\dot{\varphi}\right)\left(-z\frac{\partial \delta\dot{w}_0}{\partial x} + h_1(z)\delta\dot{\varphi}\right) + \dot{w}_0\delta\dot{w}_0\right]\mathrm{d}A\mathrm{d}x\mathrm{d}t - \\ &\int_0^T\int_0^L q\delta w_0\mathrm{d}x\mathrm{d}t, \end{aligned} \tag{9}$$

or

$$\begin{aligned} 0 = &\int_0^T\int_0^L\left\{\left(M_{xx}\delta\varepsilon_{xx}^{(1)} + S_{xx}\delta\varepsilon_{xx}^{h}\right) + Q_h\delta\gamma_{xz}^{h} - q\delta w_0 - \left[\left(I_2\frac{\partial \dot{w}_0}{\partial x} - \right.\right.\right. \\ &\left.\left.\left.I_h\dot{\varphi}\right)\frac{\partial \delta\dot{w}_0}{\partial x} + \left(-I_h\frac{\partial \dot{w}_0}{\partial x} + I_{hh}\dot{\varphi}\right)\delta\dot{\varphi} + I_0\dot{w}_0\delta\dot{w}_0\right]\right\}\mathrm{d}x\mathrm{d}t, \end{aligned} \tag{10}$$

or in the final form

$$\begin{aligned} &\int_0^T\int_0^L\left\{\left(-\frac{\partial^2 M_{xx}}{\partial x^2} - q - I_2\frac{\partial^2 \dot{w}_0}{\partial x^2} + I_h\frac{\partial \dot{\varphi}}{\partial x} + I_0\ddot{w}_0\right)\delta w_0 + \left(-\frac{\partial S_{xx}}{\partial x} + \right.\right. \\ &\left.\left.Q_h - I_h\frac{\partial \dot{w}_0}{\partial x} + I_{hh}\ddot{\varphi}\right)\delta\varphi\right\}\mathrm{d}x\mathrm{d}t + \int_0^T\left\{-M_{xx}\frac{\partial \delta\dot{w}_0}{\partial x} + \left[\frac{\partial M_{xx}}{\partial x} + \right.\right. \\ &\left.\left.I_2\frac{\partial \dot{w}_0}{\partial x} - I_h\ddot{\varphi}\right]\delta w_0 + S_{xx}\,\delta\varphi\right\}_0^L\mathrm{d}t = 0. \end{aligned} \tag{11}$$

The stress resultants M_{xx}, S_{xx} and Q_h are obtained by

$$\begin{aligned} \begin{Bmatrix} M_{xx} \\ S_{xx} \end{Bmatrix} &= \int_A \sigma_{xx}\begin{Bmatrix} z \\ h_1(z) \end{Bmatrix}\mathrm{d}z = \begin{bmatrix} D_{11} & E_{11} \\ E_{11} & E_{11}^{h} \end{bmatrix}\begin{Bmatrix} \varepsilon^{(1)} \\ \varepsilon^{h} \end{Bmatrix} - \begin{Bmatrix} M_{11}^{m} \\ S_{11}^{m} \end{Bmatrix}, \\ Q_h &= \int_A \sigma_{xz}\,h_2(z)\mathrm{d}z = E_{55}^{h}\gamma_{xz}^{h}, \end{aligned} \tag{12}$$

in which

$$\begin{Bmatrix} M_{11}^{m} \\ S_{11}^{m} \end{Bmatrix} = k_c c(t)\sum_{k=s}\int_{z_k}^{z_{k+1}}\bar{e}_{31}\begin{Bmatrix} z \\ h_1(z) \end{Bmatrix}H_z\,\mathrm{d}z = \begin{Bmatrix} \beta \\ \gamma \end{Bmatrix}\frac{\partial w_0}{\partial t}, \quad s = 1, m, k-m+1, k, \tag{13}$$

and

$$\begin{Bmatrix} D_{11} \\ E_{11} \\ E_{11}^{h} \end{Bmatrix} = \int_{-\frac{h}{2}}^{\frac{h}{2}}\bar{Q}_{11}^{(k)}\begin{Bmatrix} z^2 \\ zh_1(z) \\ [h_1(z)]^2 \end{Bmatrix}\mathrm{d}z, E_{55}^{h} = \int_{-\frac{h}{2}}^{\frac{h}{2}}\bar{Q}_{55}^{(k)}[h_2(z)]^2\mathrm{d}z. \tag{14}$$

The mass inertias I_0, I_2, I_h and I_{hh} are given as

$$\begin{Bmatrix} I_0 \\ I_2 \\ I_h \\ I_{hh} \end{Bmatrix} = \int_{-\frac{h}{2}}^{\frac{h}{2}} \rho \begin{Bmatrix} 1 \\ z^2 \\ z h_1(z) \\ [h_1(z)]^2 \end{Bmatrix} \mathrm{d}z. \tag{15}$$

The governing equations of motion are represented as

$$-\frac{\partial^2 M_{xx}}{\partial x^2} - q - I_2 \frac{\partial^2 \ddot{w}_0}{\partial x^2} + I_h \frac{\partial \ddot{\varphi}}{\partial x} + I_0 \ddot{w}_0 = 0, \tag{16}$$

$$-\frac{\partial S_{xx}}{\partial x} + Q_{hx} - I_h \frac{\partial \ddot{w}_0}{\partial x} + I_{hh} \ddot{\varphi} = 0. \tag{17}$$

By using Eqs. (12)-(15), the above system of governing equations became

$$D_{11} \frac{\partial^4 w_0}{\partial x^4} - E_{11} \frac{\partial^3 \varphi}{\partial x^3} + \beta \frac{\partial^3 w_0}{\partial x^2 \partial t} - q - I_2 \frac{\partial^2 \ddot{w}_0}{\partial x^2} + I_h \frac{\partial \ddot{\varphi}}{\partial x} + I_0 \ddot{w}_0 = 0, \tag{18}$$

$$E_{11} \frac{\partial^3 w_0}{\partial x^3} - E_{11}^h \frac{\partial^2 \varphi}{\partial x^2} + \gamma \frac{\partial^2 w_0}{\partial x \partial t} + E_{55}^h \varphi - I_h \frac{\partial \ddot{w}_0}{\partial x} + I_{hh} \ddot{\varphi} = 0. \tag{19}$$

4. Solution of the Problem

To solve the equations that describe the problem, the simply-supported boundary conditions are applied and the analytical (Navier's) solution is used. The solution is supposed as

$$\begin{aligned} w_0(x,t) &= W(t) \sin\frac{n\pi x}{L}, \\ \varphi(x,t) &= X(t) \cos\frac{n\pi x}{L}, \\ q(x,t) &= Q_n(t) \sin\frac{n\pi x}{L}. \end{aligned} \tag{20}$$

Then, substituting into Eq. (18) and Eq. (19), the system can be written as

$$\begin{bmatrix} \hat{S}_{11} & \hat{S}_{12} \\ \hat{S}_{21} & \hat{S}_{22} \end{bmatrix} \begin{Bmatrix} W \\ X \end{Bmatrix} + \begin{bmatrix} \widehat{M}_{11} & \widehat{M}_{12} \\ \widehat{M}_{21} & \widehat{M}_{22} \end{bmatrix} \begin{Bmatrix} \dot{W} \\ \dot{X} \end{Bmatrix} + \begin{bmatrix} \hat{C}_{11} & \hat{C}_{12} \\ \hat{C}_{21} & \hat{C}_{22} \end{bmatrix} \begin{Bmatrix} \ddot{W} \\ \ddot{X} \end{Bmatrix} = \begin{Bmatrix} -Q_n \\ 0 \end{Bmatrix}. \tag{21}$$

Consider $q = 0$ in Eq. (18) to achieve controlling of vibration. Suppose the solution of the system of equations in Eq. (20) as

$$W(t) = W_0 \mathrm{e}^{\lambda t}, \quad X(t) = X_0 \mathrm{e}^{\lambda t}, \tag{22}$$

where λ denotes the eigenvalue and W_0 and X_0 are arbitrary parameters. We obtain

$$\begin{vmatrix} \bar{S}_{11} & \bar{S}_{12} \\ \bar{S}_{21} & \bar{S}_{22} \end{vmatrix} = 0, \tag{23}$$

where

$$\bar{S}_{ij} = \hat{S}_{ij} + \lambda \widehat{M}_{ij} + \lambda^2 \hat{C}_{ij}, \quad i,j = 1,2, \tag{24}$$

in which the coefficients $\hat{S}_{ij}$, $\widehat{M}_{ij}$ and $\hat{C}_{ij}$ are written in Appendix B. Two sets of eigenvalues are obtained in Eq. (23) that represent the damping rate. The eigenvalue can be written as $\lambda = -\alpha + i\omega_d$ and the damping ratio ζ_n of mode n is defined [26] as

$$\zeta_n = \frac{-\alpha}{\sqrt{\alpha^2 + \omega_d{}^2}}. \tag{25}$$

By applying the following initial conditions

$$\begin{aligned} w(x,0) &= 0, \quad \dot{w}(x,0) = 1, \\ \varphi(x,0) &= 0, \quad \dot{\varphi}(x,0) = 0. \end{aligned} \tag{26}$$

The solution of equations of motion is given as

$$w(x,t) = \frac{1}{\omega_d} \mathrm{e}^{-\alpha t} \sin(\omega_d t) \sin\left(\frac{n\pi x}{L}\right). \tag{27}$$

Also, the actuation stress is

$$\sigma_1(x,t) = -k_c c(t) \bar{e}_{31}^{(m)} \frac{\partial w_0}{\partial t}. \tag{28}$$

5. Numerical Results

The vibration suppression time in the uncontrolled motion imply the time require to reduce the vibration amplitude to one-tenth. This work can be achieved by embedded the smart layers at laminated composite beam and using suitable control gain of magnetic field. The improvement in the displacement and the actuation stress is discussed according to the present theory. Numerical results for the displacement w and the actuation stress σ_1 are presented for laminated composite beam under simply-supported boundary conditions. Some numerical values of the damping coefficients, damped natural frequencies, the suppression time, and the damping ratio for symmetric laminates and antisymmetric cross-ply laminates are investigated. Additional results of the effect of lamination schemes, modes, the control gain of the magnetic field intensity and magnetostrictive layers place from the mid-plane axis on vibration suppression time are illustrated. The results of the present models are compared with those in Ref. [2]. The plots of $w(x,t)$ and $\sigma_1(x,t)$ can be displyed in the intervals $0 \le x \le 1$ and $-0.5 \le z \le 0.5$. The lamina properties of CFRP material and the magnetostrictive layer are given in Reddy and Barbosa [2] as

CFRP material:

$$E_{11} = 138.6 \text{ GPa}, \quad E_{22} = 8.27 \text{ GPa},$$
$$G_{13} = G_{23} = 0.6\, E_{22}, \quad G_{12} = 4.12 \text{ GPa},$$
$$v_{12} = 0.26, \quad \rho = 1824 \text{ kg m}^{-3}.$$

Magnetostrictive layer:

$$E_m = 26.5 \text{ GPa}, \quad \rho_m = 9250 \text{ kg},$$
$$d_k = -1.67 \times 10^{-8} \text{ m A}^{-1}, \quad c(t)k_c = 10^4,$$
$$v_m = 0, \quad L = 1 \text{ m}, \quad h_k = 1 \text{ mm}, \quad h_m = 1 \text{ mm}.$$

5.1. Symmetric angle-ply and cross-ply laminates

The controlled and uncontrolled motion for symmetric angle-ply and cross-ply laminates are studied. The damping ratio is tested, and the type of damping is determined in the system. The damping ratio is ranged in the interval $0 < \zeta_n < 1$ thus the system is underdamped while $\zeta_n = 0$ means the motion is uncontrolled. The uncontrolled motion is no appearing in any corresponding model, but it is created to purpose of the comparing and to show the effect of $c(t)k_c$ coefficient on the vibration suppression of the system. The present results are compared with those that based on ECBT, TFBT and RHBT. Some variation is found between results

of the three theories ECBT, TFBT, RHBT, and the present theory, just in the higher modes.

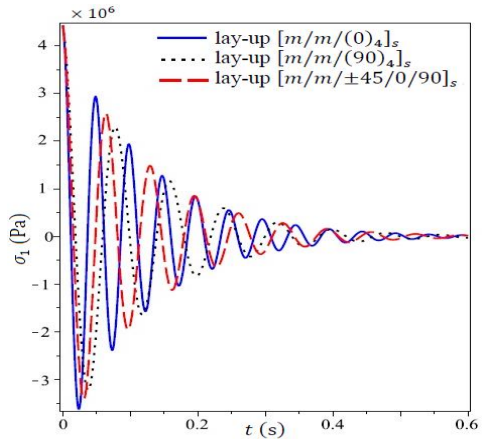

Figure 2. Maximum actuation stress ($\boldsymbol{\sigma_1}$) at the midpoint for the smart layer of various lay-ups.

The effect of the smart magnetostrictive layers location and various lamination schemes on the vibration control are displayed in Tables 1 and 2 at the first mode. It is noticeable that the value of the damping coefficient α increases and the frequency decreases in the beams therefore the damping ratio is growing whenever the layer is placed away from the mid-plane (x-axis). A lower damping ratio implies a lower decay rate, hence extremely underdamped ($\zeta_n < 1$) systems vibrate for long times. In addition, the deflection has largest value at the composite laminated beam $[m/m/90_4]_s$ that up to 12.761 mm but it represents the faster case according to the value of damping ratio that is $\zeta_n = 0.107$. The smallest deflection value occurs at the composite laminated beam $[m/m/0_4]_s$, which equals to 7.858. Hence it can be considered that the last one is the strongest beam while the first one is the weakest beam. The maximum deflection and the axial stress are located at the center of beam. The two laminates have the same maximum value of actuation stress, which up to 4.4255 MPa for each smart layer. The actuation stress distribution σ_1 for various lay-ups is illustrated in Figure 2 at the first mode.

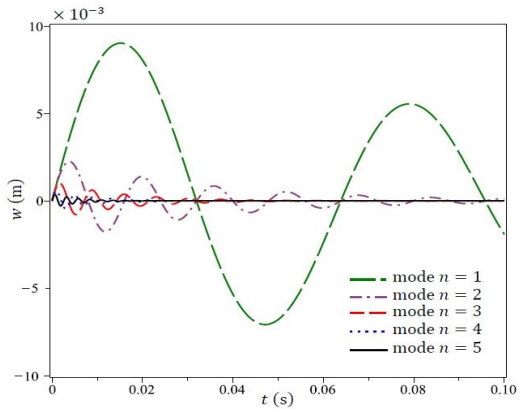

Figure 3. Controlled motion of the $[m/45/m/-45/0/90]_s$ beam for various modes at the midpoint.

The damping and frequency coefficients for symmetric angle-ply laminated composite beam with lamination scheme $[m/45/m/-45/0/90]_s$ are listed in Table 3 for transverse modes $n = 1$ to 5 based on some theories and it is shown based on the present theory in Figure 3. The higher modes give the largest value of damping rate as well it gives the largest value of the ζ_n thus the faster vibration suppression and low deflection in beams are obtained as it is illustrated from the figure.

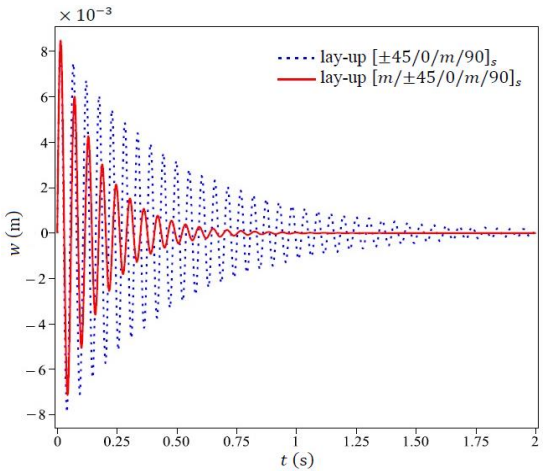

Figure 4. Effect of smart layers number on the controlled motion at the midpoint.

Figure 4 gives comparisons of the smart layer's number effect in the composite beam on the vibration control for different lay-ups using the present theory when $n = 1$. It illustrates faster vibration suppression in the beam whenever the magnetostrictive layers number is more. In Table 4 the new models are compared with those in Ref. [2] to understand the relationship between the number of smart layers in the structure and the vibration suppression time. It can be observed that the value of the damping coefficient α is increasing, and the value of the frequency is decreasing in the present models. Hence, the damping ratio increases thus implies lower vibration suppression time.

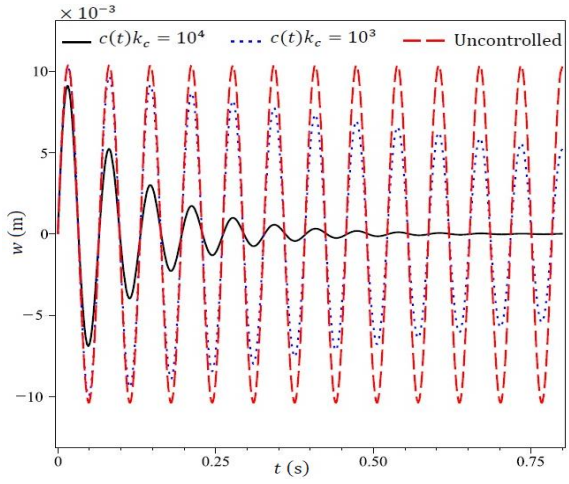

Figure 5. Effect of $\boldsymbol{c(t)k_c}$ parameter on the motion of the $[m/m/\pm45/0/90]_s$ beam at the midpoint.

Figure 5 shows the controlled and uncontrolled motion response of the beam $[m/m/\pm45/0/90]_s$ to the control gain coefficient of the applied magnetic field at the first mode according to the present theory. It is observed that salient increases in the damping coefficient and salient decreases in the damping time whenever $c(t)\ k_c$ parameter is grown. Therefore, the result is the suppression rapid for the system vibration, while the deflection increases slightly with the increase of the $c(t)\ k_c$ parameter, for more illustration see Tables 1 and 5.

cross-section.

Table 1. Suppression time for various locations of magnetostrictive layers in laminates with $c(t)k_c = 10^4$.

Lamination	$-\alpha \pm \omega_d$	$W_{\max}$	t(s)	ζ_n
$[m/\pm 45/0/90/m]_s$	5.08±108.06	9.254	0.453	0.047
$[m/\pm 45/0/m/90]_s$	5.93±108.45	9.221	0.389	0.055
$[m/\pm 45/\mathrm{m}/0/90]_s$	6.77±100.24	9.976	0.340	0.067
$[m/45/m/-45/0/90]_s$	7.62±98.41	10.162	0.302	0.077
$[m/m/\pm 45/0/90]_s$	8.46±95.91	10.426	0.272	0.088

Table 2. Suppression time for various locations of magnetostrictive layers in cross-ply laminates with $c(t)k_c = 10^4$.

Lamination	$-\alpha \pm \omega_d$	$W_{\max}$(mm)	t(s)	ζ_n
$[m/0/90/m/0/90]_s$	6.77±127.30	7.856	0.340	0.053
$[m/0/m/90/0/90]_s$	7.62±128.33	7.792	0.302	0.0593
$[m/m/0/90/0/90]_s$	8.46±114.25	8.753	0.272	0.0739
$[m/m/90_4]_s$	8.46±78.37	12.761	0.272	0.107
$[m/m/0_4]_s$	8.46±127.26	7.858	0.272	0.066

Table 3. Damping and frequency parameters of the transverse modes $-\alpha \pm \omega_d$ (rad s^{-1}) for lay-up $[m/45/\mathrm{m}/-45/0/90]_s$.

Mode	ECBT	TFBT	RHBT	Present
1	7.62±98.44	7.61±98.41	7.61±98.39	7.62±98.41
2	30.46±393.65	30.39±393.22	30.36±392.96	30.46±393.15
3	68.47±885.33	68.13±883.17	67.96±881.88	68.47±882.83
4	121.58±1572.98	120.53±1566.18	119.99±1562.16	121.58±1565.13
5	189.67±2455.90	187.13±2439.43	185.85±2429.73	189.70±2436.89

Table 4. Comparison for effect of the smart layer's number at the composite beam on the vibration control.

Lamination	$-\alpha \pm \omega_d$	$W_{\max}$	t(s)	ζ_n
$[\pm 45/0/m/90]_s$ [2]	1.98±116.85	8.558	1.163	0.017
$[\pm 45/0/m/90]_s$ (present)	1.98±116.87	8.557	1.163	0.017
$[m/\pm 45/0/m/90]_s$	5.93±108.45	9.221	0.389	0.055
$[45/m/-45/0/90]_s$ [2]	4.62±102.15	9.790	0.498	0.045
$[45/m/-45/0/90]_s$ (present)	4.62±102.16	9.788	0.498	0.045
$[m/45/m/-45/0/90]_s$	7.62±98.41	10.162	0.302	0.077
$[m/\pm 45/0/90]_s$ [2]	5.94±98.42	10.161	0.388	0.060
$[m/\pm 45/0/90]_s$ (present)	5.94±98.45	10.157	0.388	0.060
$[m/m/\pm 45/0/90]_s$	8.46±95.91	10.426	0.272	0.088

Table 5. Suppression time for various locations of magnetostrictive layers in laminates with $c(t)k_c = 10^3$.

Lamination	$-\alpha \pm \omega_d$	$W_{\max}$	$t(\mathrm{s})$	ζ_n
$[m/\pm 45/0/90/m]_s$	0.508±108.18	9.244	4.534	0.047
$[m/\pm 45/0/m/90]_s$	0.593±118.61	9.208	3.886	0.050
$[m/\pm 45/m/0/90]_s$	0.677±100.47	9.953	3.400	0.067
$[m/45/m/-45/0/90]_s$	0.762±98.70	10.132	3.023	0.077
$[m/m/\pm 45/0/90]_s$	0.846±96.28	10.386	2.720	0.088

Table 6. Suppression time and maximum deflection for various locations of magnetostrictive layers in antisymmetric cross-ply laminates with $c(t)k_c = 10^4$.

Lamination	$-\alpha \pm \omega_d$	$W_{\max}$	$t(\mathrm{s})$	ζ_n
$[m/90/0/90/0/m/m/90/0/90/0/m]$	5.08±122.50	8.163	0.453	0.0414
$[m/90/0/90/m/0/90/m/0/90/0/m]$	5.93±120.90	8.271	0.389	0.0490
$[m/90/0/m/90/0/90/0/m/90/0/m]$	6.77±117.66	8.498	0.340	0.0575
$[m/90/m/0/90/0/90/0/90/m/0/m]$	7.62±112.68	8.873	0.302	0.0675
$[m/m/(90/0/90/0)_2]$	8.46±105.68	9.46	0.272	0.0798

5.2. Antisymmetric cross-ply laminates

The effect of magnetostrictive layers location in the antisymmetric cross-ply laminates is investigated. The damping coefficient, the frequency, the suppression time and the damping ratio numerical results are listed in Table 6 for the first transverse mode according to the present theory. The same result at the symmetric laminates is observed that the suppression process directly proportional to the distance of the smart layers from the x-axis. The damping ratio increases whenever the magnetostrictive layers are located away from the mid-plane (x-axis) as well the deflection inversely proportional to the place of the smart layers from the x-axis because the frequency decreases.

6. Conclusions

This article discusses the vibration suppression at laminated composite beam embedded Terfenol-D magnetostrictive material layers, which uses to aim damping at the beams with the velocity feedback control and constant gain distributed. The Naiver analytical solution approach is applied where the beam is subjected to the boundary conditions of simply-supported. The models in Ref. [2] is used in the comparison and discussions. It is observed that the composite laminated beam with lamination scheme $[m/m/90_4]_s$ represents the weakest but it the fastest, while the composite laminated beam with lamination scheme $[m/m/0_4]_s$ represents the strongest one. In addition, the vibration suppression time is decreasing whenever the smart layers are increasing in the beam, as well the magnetostrictive layers must place far away from the x-axis to suppress vibration best. Moreover, the suppression time and deflection value are inversely proportional to the control gain coefficient $c(t)k_c$ of the applied magnetic field.

7. Appendix A

The coefficients $\bar{Q}_{ij}^{(k)}$ appeared in Eqs. (4) and (5) are given by

$$\bar{Q}_{11}^{(k)} = Q_{11}^{(k)}\cos^4\theta^{(k)} + 2\left(Q_{12}^{(k)}+2Q_{66}^{(k)}\right)\cos^2\theta^{(k)}\sin^2\theta^{(k)} + Q_{22}^{(k)}\sin^4\theta^{(k)},$$

$$\bar{Q}_{55}^{(k)} = Q_{55}^{(k)}\cos^2\theta^{(k)} + Q_{44}^{(k)}\sin^2\theta^{(k)},$$

$$\bar{Q}_{13}^{(k)} = Q_{13}^{(k)}\cos^2\theta^{(k)} + Q_{23}^{(k)}\sin^2\theta^{(k)},$$

$$\bar{Q}_{33}^{(k)} = Q_{33}^{(k)},$$

$$Q_{11}^{(k)} = \frac{1-\nu_{23}^{(k)}\nu_{32}^{(k)}}{E_{22}^{(k)}E_{33}^{(k)}\Delta}, \quad Q_{12}^{(k)} = \frac{\nu_{21}^{(k)}+\nu_{31}^{(k)}\nu_{23}^{(k)}}{E_{22}^{(k)}E_{33}^{(k)}\Delta} = \frac{\nu_{12}^{(k)}+\nu_{13}^{(k)}\nu_{32}^{(k)}}{E_{11}^{(k)}E_{33}^{(k)}\Delta},$$

$$Q_{22}^{(k)} = \frac{1-\nu_{13}^{(k)}\nu_{31}^{(k)}}{E_{11}^{(k)}E_{33}^{(k)}\Delta}, \quad Q_{13}^{(k)} = \frac{\nu_{31}^{(k)}+\nu_{21}^{(k)}\nu_{32}^{(k)}}{E_{22}^{(k)}E_{33}^{(k)}\Delta} = \frac{\nu_{13}^{(k)}+\nu_{12}^{(k)}\nu_{23}^{(k)}}{E_{11}^{(k)}E_{22}^{(k)}\Delta},$$

$$Q_{23}^{(k)} = \frac{\nu_{32}^{(k)}+\nu_{12}^{(k)}\nu_{31}^{(k)}}{E_{11}^{(k)}E_{33}^{(k)}\Delta} = \frac{\nu_{32}^{(k)}+\nu_{21}^{(k)}\nu_{13}^{(k)}}{E_{11}^{(k)}E_{33}^{(k)}\Delta}, \quad Q_{33}^{(k)} = \frac{1-\nu_{12}^{(k)}\nu_{21}^{(k)}}{E_{11}^{(k)}E_{22}^{(k)}\Delta},$$

$$Q_{44}^{(k)} = G_{23}^{(k)}, \quad Q_{55}^{(k)} = G_{31}^{(k)}, \quad Q_{66}^{(k)} = G_{12}^{(k)},$$

$$\Delta = \frac{1-\nu_{12}^{(k)}\nu_{12}^{(k)}-\nu_{23}^{(k)}\nu_{32}^{(k)}-\nu_{13}^{(k)}\upsilon^{(k)}{}_{31}-2\nu_{21}^{(k)}\nu_{13}^{(k)}\nu_{32}^{(k)}}{E_{11}^{(k)}E_{22}^{(k)}E_{33}^{(k)}},$$

$$\nu_{21}^{(k)} = \nu_{12}^{(k)}E_{11}^{(k)}E_{22}^{(k)}, \quad \nu_{31}^{(k)} = \nu_{13}^{(k)}\frac{E_{33}^{(k)}}{E_{11}^{(k)}}, \quad \nu_{32}^{(k)} = \nu_{13}^{(k)}\frac{E_{33}^{(k)}}{E_{22}^{(k)}},$$

where E_i are Young's moduli in the material principal directions, ν_{ij} are Poisson's ratios and G_{ij} are the moduli of shear.

8. Appendix B

The components of the coefficients $\hat{S}_{ij}$, $\widehat{M}_{ij}$ and $\hat{C}_{ij}$ $(i = 1,2)$ appeared in Eq. (21) can be written as

$$\hat{S}_{11} = D_{11}\left(\frac{n\pi}{L}\right)^4, \ \hat{S}_{12} = -E_{11}\left(\frac{n\pi}{L}\right)^3,$$

$$\hat{S}_{21} = -E_{11}\left(\frac{n\pi}{L}\right)^3, \ \hat{S}_{22} = E_{11}^{\mathrm{h}}\left(\frac{n\pi}{L}\right)^2 + E_{55}^{\mathrm{h}},$$

$$\widehat{M}_{11} = -\beta\left(\frac{n\pi}{L}\right)^2, \quad \widehat{M}_{21} = \gamma\frac{n\pi}{L}, \quad \widehat{M}_{12} = 0, \quad \widehat{M}_{22} = 0,$$

$$\hat{C}_{11} = I_2\left(\frac{n\pi}{L}\right)^2 + I_0, \quad \hat{C}_{12} = -I_h\frac{n\pi}{L}, \quad \hat{C}_{22} = I_{hh}.$$

References

1. Goodfriend M.J, Shoop K.M., 1992, Adaptive characteristics of the magnetostrictive alloy, Terfenol-D, for active vibration control, Journal of Intelligent Material Systems and Structures 3: 245-254.
2. Reddy J.N., Barbosa J.I., 2000, On vibration suppression of magnetostrictive beams, Smart Materials and Structures 9: 49-58.
3. Reddy J.N., 1997, Mechanics of Laminated Composite Plates: Theory and Analysis, CRC Press, Boca Raton, FL.
4. Murty A.V.K., Anjanappa M., Wu Y-F., Bhattacharya B., Bhat M.S., 1998, Vibration suppression of laminated composite beams using embedded magnetostrictive layers, Institution of Engineers (India) Journal of Aerospace 78: 38-44.
5. Pradhan S.C., Ng T.Y., Lam K.Y., Reddy J.N., 2001, Control of laminated composite plates using magnetostrictive layers, Smart Materials and Structures 10: 1-11.
6. Kumar J.S., Ganesan N., Swarnamani S., Padmanabhan C., 2004, Active control of simply supported plates with a magnetostrictive layer, Smart Materials and Structures 13(3): 487-492.
7. Zhang Y., Zhou H., Zhou Y., 2015, Vibration suppression of cantilever laminated composite plate with nonlinear giant magnetostrictive material layers, Acta Mechanica Solida Sinca 28: 50-60.
8. Subramanian P., 2002, Vibration suppression of symmetric laminated composite beams, Smart Materials and Structures 11(6): 880–885.
9. Kumar J.S., Ganesan N., Swarnamani S., Padmanabhan C., 2003, Active control of beam with magnetostrictive layer, Computers and Structures 81(13): 1375-1382.
10. Ghosh D.P., Gopalakrishnan S., 2005, Coupled analysis of composite laminate with embedded magnetostrictive patches, Smart Materials and Structures 14(6): 1462-1473.
11. Zhou H.M., Zhou Y.H., 2007, Vibration suppression of laminated composite beams using actuators of giant magnetostrictive materials, Smart Materials and Structures 16(1): 198-206.
12. Murty A.V.K., Anjanappa M., Wu Y-F, 1997, The use magnetostrictive particle actuators for vibration attenuation of flexible beams, Journal of Sound and Vibrations 206(2): 133-149.
13. Lee S.J., Reddy J.N., Rostam-Abadi F., 2004, Transient analysis of laminated composite plates with embedded smart-material layers, Finite Elements in Analysis and Design 40(5-6): 463-483.
14. Snowdon J.N., 1968, Vibration and Shock in Damped Mechanical Systems, Wiley, New York.
15. Rostam-Abadi F., Reddy J.N., Lee S.J., 2002, Vibration suppression of cross-ply laminated plates with magnetostrictive layers, Proceedings of SECTAM XXI.
16. Reddy J.N., 2002, Energy Principles and Variational Methods in Applied Mechanics, Wiley, New York.
17. Hiller M.W., Bryant M.D., Umegaki J., 1989, Attenuation and transformation of vibration through active control of magnetostrictive Terfenol, Journal of Sound and Vibrations 134: 507-519.
18. Pratt J.R., Flatau A.B., 1995, Development and analysis of self-sensing magnetostrictive actuator design Journal of Intelligent Material Systems and Structures 6: 639-648.
19. Anjanappa M., Bi J., 1993, Modelling, design and control of embedded Terfenol-D actuator, Smart Structures and Intelligent Systems 1917: 908-918.
20. Anjanappa M., Bi J., 1994, A theoretical and experimental study of magnetostrictive mini actuators, Smart Materials and Structures 1: 83-91.
21. Arani A.G., Maraghi Z.K., 2016, A feedback control system for vibration of magnetostrictive plate subjected to follower force using sinusoidal shear deformation theory, Ain Shams Engineering Journal 7(1): 361-369.
22. Reddy J.N., 1999, On laminated composite plates with integrated sensors and actuators, Engineering Structures 21(7): 568-593.
23. Koconis D.B., Kollar L.P., Springer G.S., 1994, Shape control of composite plates and shells with embedded actuators I: voltage specified, Journal of Composite Materials 28: 415-458.
24. Shankar G., Kumar S.K., Mahato P.K., 2017, Vibration analysis and control of smart composite plates with delamination and under hygrothermal environment, Thin-Walled Structures 116: 53-68.
25. Arani A.G., Maraghi Z.K., Arani H.K., 2017, Vibration control of magnetostrictive plate under multi-physical loads via trigonometric higher order shear deformation theory, Journal of Vibration and Control 23(19): 3057-3070.
26. Li J., Ma Z., Wang Z., Narita Y., 2016, Random vibration control of laminated composite plates with piezoelectric fiber reinforced composites, Acta Mechanica Solida Sinca 29(3): 316-327.
27. Zenkour A.M., 2015, Thermal bending of layered composite plates resting on foundations using four-unknown shear and normal deformations theory, Composite Structures 122: 260-270.
28. Li J., Narita Y., 2013, Vibration suppression for laminated composite plates with arbitrary boundary conditions, Mechanics of Composite Materials 49(5): 519-530.
29. Song G., Qiao P.Z., Binienda W.K., Zou G.P., 2002, Active vibration damping of composite beam using smart sensors and actuators, Journal of Aerospace Engineering 15(3): 97-103.
30. Kim H.S., Sohn J.W., Choi S.B., 2011, Vibration control of a cylindrical shell structure using macro fiber composite actuators, Mechanics Based Design of Structures and Machines 39(4): 491-506.
31. Touratier M., 1991, An efficient standard plate theory, International Journal of Engineering Science 29(8): 901-916.
32. Zenkour A.M., 2013, Bending analysis of functionally graded sandwich plates using a simple four-unknown shear and normal deformations theory, Journal of Sandwich Structures and Materials 15(6): 629-656.
33. Zenkour A.M., 2013, A simple four-unknown refined theory for bending analysis of functionally graded plates, Applied Mathematical Modelling 37(20-21): 9041-9051.
34. Zenkour A.M., 2013, Bending of FGM plates by a simplified four-unknown shear and normal deformations theory, International Journal of Applied Mechanics 5(2): 1350020, 1-15.
35. Al Khateeb S.A., Zenkour A.M., 2014, A refined four-unknown plate theory for advanced plates resting on elastic foundations in hygrothermal environment, Composite Structures 111(1): 240-248.
36. Zenkour A.M., 2015, A simplified four-unknown shear and normal deformations theory for bidirectional laminated plates, Sādhanā 40(1): 215-234.
37. Bouazza M., Zenkour A.M., N. Benseddiq, 2018, Closed-from solutions for thermal buckling analyses of advanced nanoplates according to a hyperbolic four-variable refined theory with small-scale effects, Acta Mechanica 229(5): 2251-2265.
38. Farajpour A., Yazdi M.R.H., Rastgoo A., Loghmani M., Mohammadi M., 2016, Nonlocal nonlinear plate model for large amplitude vibration of magneto-electro-elastic nanoplates, Composite Structures 140: 323-336.